A Letters Journal Exploring the Frontiers of Physics

July 2009

EPL, **87** (2009) 28002
doi: 10.1209/0295-5075/87/28002

www.epljournal.org

Enhancement of the processivity of kinesin-transported cargo by myosin V

F. Berger[a], M. J. I. Müller and R. Lipowsky

Max Planck Institute of Colloids and Interfaces - 14424 Potsdam, Germany, EU

received 19 March 2009; accepted in final form 30 June 2009
published online 29 July 2009

PACS 87.16.Nn – Motor proteins (myosin, kinesin, dynein)
PACS 87.15.hj – Biomolecules: structure and physical properties: Transport dynamics
PACS 87.10.Mn – Biological and medical physics: Stochastic modeling

Abstract – Intracellular transport by molecular motors proceeds in two steps: long-range transport along microtubules and local delivery via actin filaments. A recent *in vitro* experiment has revealed that the actin-based motor myosin V can diffuse along microtubules and can enhance the processivity of cargos pulled by the microtubule-based motor kinesin-1 (Ali M. Y. *et al.*, *Proc. Natl. Acad. Sci. U.S.A.*, **105** (2008) 4691). Here we present a stochastic model for cargo transport by a directional motor (kinesin) and a diffusing motor (myosin). By using a subset of the experimental data of Ali *et al.* to adjust our model parameters, we are able to describe all experimental results. In our model, the myosins do not influence kinesin's motion and only act as tethers which allow the kinesin to rebind. Furthermore we find that the run length of the cargo increases exponentially with the number of myosins.

Introduction. – The complex internal structure of cells depends, to a large extent, on active transport by molecular motors [1]. These proteins can be viewed as "nano-trucks" that transport cellular cargo along "roads" formed by cytoskeletal filaments. These filaments are polar with a plus and a minus end, which can be recognized by the motors so that a single motor can walk along the filament in a directed way. Since motors constantly undergo thermal collisions with surrounding molecules, they unbind from their track after a finite run length, which is of the order of μm for typical processive motors [2].

There are two types of filaments: microtubules, which form long highways from the cell center to the cell periphery, and shorter actin filaments, which act as a dense meshwork of side roads mainly in the cell periphery. Cellular transport is based on both types of filaments and accomplished in two steps: long-range transport is mediated by the microtubule-based kinesin and dynein motors, while local delivery is the task of the actin-based myosin motors [3–5].

During this "dual transport", cargos must be able to switch from the microtubule to the actin track, as has indeed been observed for various cellular cargos such as mitochondria, pigment granules and synaptic vesicles, reviewed in [4,5]. These cargos are attached to both myosin and kinesin motors, as depicted in fig. 1(a). The simplest scenario for such cargo transport is that, during microtubule-based motion, myosin is not bound to the microtubule but is simply riding piggyback on the cargo pulled by kinesin, and vice versa for kinesin during actin-based motion. However, recent *in vitro* experiments by Ali *et al.* [6,7] suggest that there might be a more useful role for the non-active motor: They have shown that myosin V binds to microtubules and diffuses randomly on

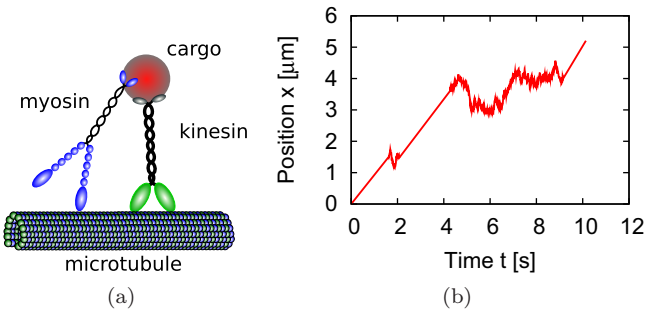

(a) (b)

Fig. 1: (Colour online) (a) A cargo particle is attached to a microtubule by $N_k = 1$ kinesin and $N_m = 1$ myosin motor; (b) a typical simulated trajectory of a cargo particle transported by one kinesin and one myosin.

[a]E-mail: florian.berger@mpikg.mpg.de

them, and that kinesin-1 weakly binds to actin filaments. Furthermore, they demonstrated that cargos transported by myosin and kinesin simultaneously exhibit longer run lengths before unbinding from the filament [7]. They explain their findings with the intuitive idea that the diffusing motor tethers the cargo to the filament even when the active motor unbinds, so that the active motor has a chance to rebind to the filament and continue cargo transport [7]. However, the precise coordination mechanism of the two motors remains to be elucidated.

In this paper, we present a stochastic model for the transport of a single cargo by actively pulling and passively tethering motors. We apply this general model to the case of transport by one myosin and one kinesin along a microtubule, as considered in the *in vitro* experiment in ref. [7]. Each motor stochastically binds to and unbinds from the filament. When bound, the kinesin actively walks into one direction, while myosin diffuses randomly along the filament. We deduce the rates for these stochastic events from a subset of the experimental data, and then use our model to describe all experimentally measured quantities, finding good quantitative agreement. We also investigate the effect of several myosins on a cargo pulled by a single kinesin, which leads to an exponential increase of the cargo's run length.

Our model uses the same theoretical framework as previous models for cargo transport by several molecular motors of one species [8] and of two species walking into opposite directions [9,10]. These models describe cargo transport by a few motors on the length scale of a few to tens of μm, taking into account the fluctuations of the number of bound motors, as is appropriate for intracellular transport as well as for the *in vitro* experiment considered here. They are therefore useful on length scales intermediate between single-motor walks of a few μm, and effective random walks of the cargo on cellular length scales [11–13].

Theoretical model. – In our model, a cargo is attached to a fixed number of N_k kinesins and N_m myosins, see fig. 1(a). In the experiment of ref. [7], only one kinesin was bound to the cargo particle, a 10 nm sized quantum dot. The precise number of attached myosins was unknown; however, the small size of the cargo suggests that only a single myosin was attached to it. Therefore, we first focus on the case of $N_\mathrm{k} = N_\mathrm{m} = 1$, and discuss the general case of $N_\mathrm{m} > 1$ at the end of this article.

Since the motors stochastically bind to and unbind from the filament, a cargo transported by one kinesin and one myosin can be in one of four possible states $(n_\mathrm{m}, n_\mathrm{k})$ characterized by the numbers n_m and n_k of bound myosins and kinesins, respectively, see fig. 2(a). In state $(1,0)$ only myosin is bound and in state $(0,1)$ only kinesin. Both motors are bound to the filament in state $(1,1)$. The state $(0,0)$ refers to the case when both motors are unbound. Stochastic motor binding and unbinding events correspond to transitions between the four states,

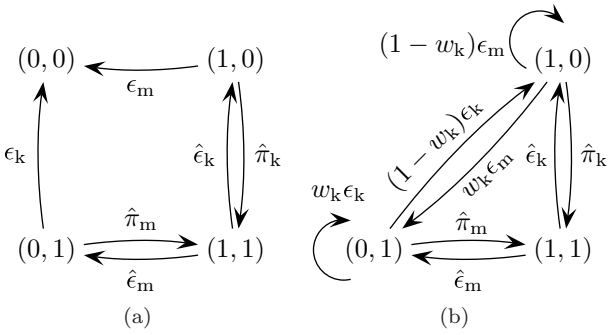

Fig. 2: (a) State space of a cargo particle transported by one kinesin and one myosin. The particle can be bound to the microtubule by kinesin only (state $(0,1)$), myosin only (state $(1,0)$), or both motors (state $(1,1)$), or be in the unbound state $(0,0)$. Stochastic motor unbinding and binding transitions with rates ϵ_k, ϵ_m, etc., lead to a random walk on this space of four cargo states; (b) closed network obtained from (a) by redirecting all arrows that lead into the absorbing state $(0,0)$ back into the states $(0,1)$ and $(1,0)$, weighted with the respective probabilities w_k and $(1-w_\mathrm{k})$.

Table 1: Single-motor parameters for kinesin-1 (kin.) and myosin V (myo.) of the model defined in fig. 2(a). Values with asterisk were determined from the experiments in ref. [7]. The other values were deduced from our model as described in the text.

kin. parameter		sym.	value
binding rate	bound myo.	$\hat{\pi}_\mathrm{k}$	0.20/s
unbinding rate	no myo.	ϵ_k	0.52/s*
unbinding rate	bound myo.	$\hat{\epsilon}_\mathrm{k}$	0.52/s
velocity		v_k	0.88 μm/s*
myo. parameter		**sym.**	**value**
binding rate	bound kin.	$\hat{\pi}_\mathrm{m}$	0.25/s
unbinding rate	no kin.	ϵ_m	0.020/s*
unbinding rate	bound kin.	$\hat{\epsilon}_\mathrm{m}$	0.12/s
diff. constant	no kin.	D_m	0.18 μm^2/s*

as indicated by arrows in fig. 2(a). The rates associated with these transitions are listed in table 1.

In state $(0,1)$ with only kinesin bound, the cargo is pulled with the kinesin velocity v_k, which equals 0.88 μm/s in the experiment of ref. [7]. Since single myosins diffuse randomly on microtubules, a cargo in state $(1,0)$ moves on average with zero velocity. The myosin diffusion constant $D_\mathrm{m} \simeq 0.18\,\mu\mathrm{m}^2/\mathrm{s}$ [7] corresponds to a friction coefficient $\gamma_\mathrm{m} = k_\mathrm{B}T/D_\mathrm{m} \simeq 0.02\,\mathrm{pNs}/\mu\mathrm{m}$ for motion of myosin on microtubules. When kinesin and myosin are both bound the moving kinesin experiences a rather small friction coefficient. It can easily drag the myosin along when moving with its velocity $v_\mathrm{k} \simeq 0.88\,\mu$m/s, since the myosin friction force $\gamma_\mathrm{m} v_\mathrm{k}$ is only about 0.02 pN and thus negligible for kinesin with a stall force of about 6–7 pN [14,15]. Therefore we assume that a cargo in state $(1,1)$ moves with velocity v_k.

In the experiments of ref. [7], cargos were monitored starting immediately after they bind to the microtubule and ending when they unbound from it. Since it is unlikely that both motors bind to the filament at the same time when the cargo binds to the filament from the surrounding solution, the cargo starts its run on the microtubule either in the state $(n_{\rm m}, n_{\rm k}) = (0,1)$ with only kinesin bound, or in the state $(1,0)$ with only myosin bound. We expect that the probability for a "kinesin start" in state $(0,1)$, which we denote as $w_{\rm k}$, is much higher than the probability $(1-w_{\rm k})$ for a "myosin start" in $(1,0)$ since the affinity of kinesin for microtubules is much higher than that of the actin motor myosin. Cargo unbinding corresponds to the transitions to the unbound state $(0,0)$. Since the cargo then performs diffusive motion away from the filament, the state $(0,0)$ is an absorbing state of the network in fig. 2(a).

In total, a cargo with one myosin and one kinesin stochastically switches between the four states displayed in fig. 2(a). The cargo trajectory in physical space consists of alternating sequences of directed motion with the kinesin velocity $v_{\rm k}$ when the cargo is in the kinesin states $(0,1)$ and $(1,1)$, and random diffusive motion when the cargo is in the myosin state $(1,0)$. Similar to the experimental trajectories, our model trajectory in fig. 1(b) exhibits alternating "stepping events", in which the cargo moves with kinesin velocity $v_{\rm k} \simeq 0.88\,\mu$m/s and "diffusive events" in which the cargo diffuses along the filament.

Specification of model parameters. – To specify the parameters of our model from the experimental data, we derive analytical expressions for averaged quantities measured in the experiments, such as the average run length or the average duration of stepping events.

In order to calculate such quantities, we use a generalization of a method proposed by Hill [16,17]. We will explain this method for the calculation of the average run time $\langle \Delta t_{\rm ca} \rangle$, which is the average time to absorption in state $(0,0)$. The time $\langle \Delta t_{\rm ca} \rangle$ can be determined by averaging the run times of an ensemble of trajectories, each of which starts at time $t=0$ in state $(0,1)$ with probability $w_{\rm k}$ and in state $(1,0)$ with probability $(1-w_{\rm k})$. If one concatenates these trajectories, one obtains a single trajectory which, upon reaching the absorbing state $(0,0)$, immediately continues at state $(0,1)$ with probability $w_{\rm k}$, or at state $(1,0)$ with probability $(1-w_{\rm k})$. The network that describes such a trajectory is shown in fig. 2(b), which is constructed by "closing" the network of fig. 2(a), *i.e.* by eliminating the absorbing state $(0,0)$ and redirecting all arrows that ended in $(0,0)$ to the starting states. For example, the arrow from state $(0,1)$ to state $(0,0)$ with rate $\epsilon_{\rm k}$ is redirected to state $(0,1)$ with the probability weight $w_{\rm k}$ and to state $(1,0)$ with probability weight $(1-w_{\rm k})$. The stationary probabilities $P(n_{\rm m}, n_{\rm k})$ of the closed network can be calculated by matrix methods [18] or using a diagrammatic method [19,20], which leads to

$$P(0,1) \equiv \left[\hat{\epsilon}_{\rm m}\hat{\pi}_{\rm k} + \epsilon_{\rm m} w_{\rm k}(\hat{\epsilon}_{\rm k} + \hat{\epsilon}_{\rm m})\right]/\Omega, \tag{1}$$

$$P(1,0) \equiv \left[\hat{\epsilon}_{\rm k}\hat{\pi}_{\rm m} + (1-w_{\rm k})\epsilon_{\rm k}(\hat{\epsilon}_{\rm k} + \hat{\epsilon}_{\rm m})\right]/\Omega, \tag{2}$$

$$P(1,1) \equiv \left[(1-w_{\rm k})\epsilon_{\rm k}\hat{\pi}_{\rm k} + \hat{\pi}_{\rm m}(\hat{\pi}_{\rm k} + \epsilon_{\rm m} w_{\rm k})\right]/\Omega, \tag{3}$$

where Ω is determined by the normalization condition $P(0,1) + P(1,0) + P(1,1) = 1$. In the steady state the average rate of arrivals at state $(0,0)$ is given by the probability current $J \equiv \epsilon_{\rm m} P(1,0) + \epsilon_{\rm k} P(0,1)$, see fig. 2(b). For the open network in fig. 2(a), this arrival rate corresponds to the average rate of absorptions in $(0,0)$. Thus, the average time between absorptions is given by

$$\langle \Delta t_{\rm ca} \rangle \equiv 1/J = 1/\left[\epsilon_{\rm m} P(1,0) + \epsilon_{\rm k} P(0,1)\right]. \tag{4}$$

This average absorption time can also be calculated for the open network in fig. 2(a) using the general theory of Markov processes. The latter calculation confirms the expression (4) and provides a nontrivial check of our approach.

The probability $P(n_{\rm m}, n_{\rm k})$ gives the average fraction of time spent in state $(n_{\rm m}, n_{\rm k})$ per run [16]. Since there is no cargo displacement in the state $(1,0)$, the cargo moves only in the kinesin-bound states $(0,1)$ and $(1,1)$, *i.e.* during the time $[P(0,1) + P(1,1)]\langle \Delta t_{\rm ca} \rangle$. Since it moves with velocity $v_{\rm k}$ in these states, the average run length is

$$\langle \Delta x_{\rm ca} \rangle \equiv v_{\rm k}[P(0,1) + P(1,1)]\langle \Delta t_{\rm ca} \rangle = v_{\rm k} \frac{\hat{\pi}_{\rm k}(\epsilon_{\rm k} + \hat{\epsilon}_{\rm m} + \hat{\pi}_{\rm m}) + w_{\rm k}(\epsilon_{\rm m}(\hat{\epsilon}_{\rm k} + \hat{\epsilon}_{\rm m} + \hat{\pi}_{\rm m}) - \epsilon_{\rm k}\hat{\pi}_{\rm k})}{\epsilon_{\rm k}\hat{\epsilon}_{\rm m}(\epsilon_{\rm m} + \hat{\pi}_{\rm k}) + \epsilon_{\rm m}\hat{\epsilon}_{\rm k}(\epsilon_{\rm k} + \hat{\pi}_{\rm m})}. \tag{5}$$

Next, we calculate the average time $\langle \Delta t_{\rm se} \rangle$ of a stepping event, *i.e.* the average time spent continuously in the stepping states $(0,1)$ and $(1,1)$. In the open network in fig. 2(a), a stepping event can start from $(0,1)$ or from $(1,1)$. We first determine the probability $p_{1,1}$ for a stepping event to start in state $(1,1)$. The average number of transitions from $(1,0)$ to $(1,1)$ per unit time in the network of fig. 2(b) is given by the probability current $J_k(1,1) \equiv \hat{\pi}_{\rm k} P(1,0)$. Since a stepping event which starts in state $(0,1)$ can only occur at the begining of a run, the average number of these latter events per unit time in the network of fig. 2(b) corresponds to the probability current $J_k(0,1) \equiv w_{\rm k}\epsilon_{\rm k} P(0,1) + w_{\rm k}\epsilon_{\rm m} P(1,0)$ from $(0,1)$ and $(1,0)$ to $(0,1)$. This is exactly the sum of the redirected currents which represent a new run starting in state $(0,1)$. Hence the probability for a stepping event to start in state $(1,1)$ has the form

$$p_{1,1} \equiv \frac{J_k(1,1)}{J_k(1,1) + J_k(0,1)}. \tag{6}$$

A stepping event is finished when the diffusive state $(1,0)$ or the unbound state $(0,0)$ in the network of fig. 2(a) is reached. We therefore promote the state $(1,0)$ to an absorbing state, so that we now have the two absorbing states $(0,0)$ and $(1,0)$, see fig. 3(a). By redirecting all arrows from the absorbing states $(0,0)$ and $(1,0)$ to the starting states $(1,1)$ and $(0,1)$, we obtain the network in

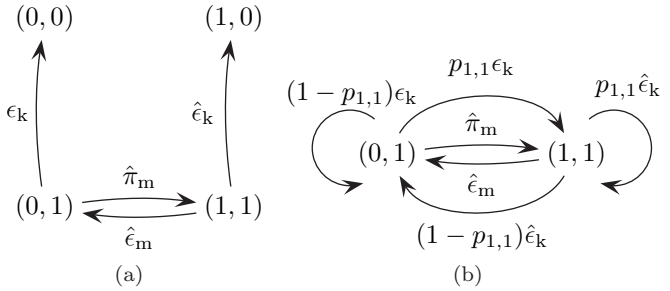

Fig. 3: (a) Network modified from fig. 2(a) with absorbing states $(0,0)$ and $(1,0)$; (b) closed network obtained from (a) by redirecting the arrows into the absorbing states (0, 0) and (1, 0). The transitions are weighted with the probability $p_{1,1}$ to start in state $(1,1)$ and $1-p_{1,1}$ to start in state $(0,1)$.

fig. 3(b). Using the stationary probabilities for the latter network, as given by

$$Q(0,1) \equiv \frac{\hat{\epsilon}_m + \hat{\epsilon}_k(1-p_{1,1})}{\hat{\epsilon}_k(1-p_{1,1}) + p_{1,1}\epsilon_k + \hat{\pi}_m + \hat{\epsilon}_m}, \tag{7}$$

$$Q(1,1) \equiv 1 - Q(0,1), \tag{8}$$

and the probability $p_{1,1}$ as in eq. (6), the average time of a stepping event is

$$\langle \Delta t_{se} \rangle \equiv \frac{1}{\epsilon_k Q(0,1) + \hat{\epsilon}_k Q(1,1)} = \frac{A+B}{\epsilon_k A + \hat{\epsilon}_k B} \tag{9}$$

with $A \equiv w_k\epsilon_m\hat{\epsilon}_k + w_k\epsilon_m\hat{\epsilon}_m + \hat{\pi}_k\hat{\epsilon}_m$ and $B \equiv w_k\epsilon_m\hat{\pi}_m + \hat{\pi}_k\hat{\pi}_m + (1-w_k)\hat{\pi}_k\epsilon_k$, in analogy with eq. (4).

Another quantity of interest is the fraction ϕ_{nde} of runs with no diffusive events. All of these runs start in state $(0,1)$, and leave the network of fig. 2(a) with the transition to state $(0,0)$ without ever visiting state $(1,0)$. Equivalently, we may ask for the probability of starting in state $(0,1)$ in the network of fig. 3(a) and being absorbed in state $(0,0)$ rather than in state $(1,0)$. This splitting probability $q_{0,0}$ is given by the ratio of the probability current from state $(0,1)$ to $(0,0)$ and the total probability current out of the network [17,19],

$$q_{0,0} \equiv \epsilon_k Q(0,1)/[\epsilon_k Q(0,1) + \hat{\epsilon}_k Q(1,1)]. \tag{10}$$

Since we now consider only runs that start in state $(0,1)$, we use the relations (7) and (8) with $p_{1,1} = 0$. Finally, we have to take into account that only the fraction w_k of runs in the original network in fig. 2(a) can contribute to runs without diffusive events. Therefore, the fraction of these latter runs is found to be

$$\phi_{nde} = w_k q_{0,0} = w_k \frac{\epsilon_k(\hat{\epsilon}_k + \hat{\epsilon}_m)}{\epsilon_k(\hat{\epsilon}_k + \hat{\epsilon}_m) + \hat{\epsilon}_k\hat{\pi}_m}. \tag{11}$$

Finally, we calculate the average time $\langle \Delta t_{de} \rangle$ of a diffusive event. Since only $(1,0)$ is a diffusive state, the average waiting time $\langle \Delta t_{de} \rangle$ in this state is given by

$$\langle \Delta t_{de} \rangle = 1/(\epsilon_m + \hat{\pi}_k). \tag{12}$$

We have now obtained analytical expressions for the average run length $\langle \Delta x_{ca} \rangle$, the average time $\langle \Delta t_{se} \rangle$ of stepping events, the average time $\langle \Delta t_{de} \rangle$ of diffusive events, and the fraction ϕ_{nde} of runs without diffusive events.

Combining these analytical results with the experimental data of ref. [7], we determine all six rates of our model in fig. 2(a). From different single-molecule experiments with $(N_m, N_k) = (0,1)$ and $(N_m, N_k) = (1,0)$, the unbinding rates of myosin ϵ_m and kinesin ϵ_k can directly be derived as the inverse of the average binding time 1.93 s of kinesin and 50 s of myosin on microtubules [7]. From the measured average time 4.5 s of a diffusive event we obtain with eq. (12) the binding rate $\hat{\pi}_k \simeq 0.2/\text{s}$. In the experiments the average time $\langle \Delta t_{se} \rangle$ of a stepping event has the same value for $(N_m, N_k) = (0,1)$ and $(N_m, N_k) = (1,1)$ and is equal to the time $1/\epsilon_k$. Therefore, we deduce from eq. (9) that the unbinding rate $\hat{\epsilon}_k$ is equal to the unbinding rate ϵ_k so that kinesin unbinding is not affected by the presence of myosin.

Since we expect that the microtubule binding affinity for kinesin is much larger than for myosin, we assume, for the moment, that all runs start in the state $(0,1)$ with kinesin bound, *i.e.* $w_k = 1$. With the measured average run length of 3.7 μm and the fact that 72% of the runs did not show diffusive events, we obtain from eq. (5) and (11) with $w_k = 1$ the rates $\hat{\pi}_m \simeq 0.25/\text{s}$ and $\hat{\epsilon}_m \simeq 0.12/\text{s}$. Note that the myosin unbinding rate $\hat{\epsilon}_m$ in the presence of bound kinesin is larger than the unbinding rate $\epsilon_m \simeq 0.02/\text{s}$ of myosin alone. Thus, kinesin acts to detach the myosin from the microtubule.

Comparison with experiments. – We have now determined all parameters needed in our model by using a subset of the experimental data of ref. [7]. These parameters are listed in table 1. We now use our model to describe all results measured in ref. [7]. In order to do so, we simulate the system depicted in fig. 2(a) with a discrete time algorithm. In state $(0,1)$, the cargo performs a discrete time continuous space random walk with the myosin diffusion constant D_m. In states $(1,0)$ and $(1,1)$, the cargo moves with a velocity chosen according to a Gaussian distribution with average value $v_k \simeq 0.88\,\mu\text{m/s}$ and standard deviation $0.2\,\mu\text{m/s}$, as determined in the experiment ref. [7]. A sample trajectory of our simulation is shown in fig. 1(b); it exhibits alternating sequences of diffusive and stepping events, and is remarkably similar to the experimental trajectories, shown in ref. [7].

First, these simulations reproduce the experimental values that we used to determine the model parameters, namely the run length $\langle \Delta x_{ca} \rangle \simeq 3.7\,\mu\text{m}$, the stepping time $\langle \Delta t_{se} \rangle \simeq 1.93\,\text{s}$, the fraction of runs without diffusive events $\phi_{nde} \simeq 0.72$ and the diffusive time $\langle \Delta t_{de} \rangle \simeq 4.5\,\text{s}$ in agreement with (5), (9), (11), (12). Second, we find i) that the average length of runs which exhibit at least one diffusive event is 9.83 μm, which is comparable to the experimental value of $7.1 \pm 1.7\,\mu\text{m}$, and ii) that the average velocities of all runs and of runs with diffusive events in

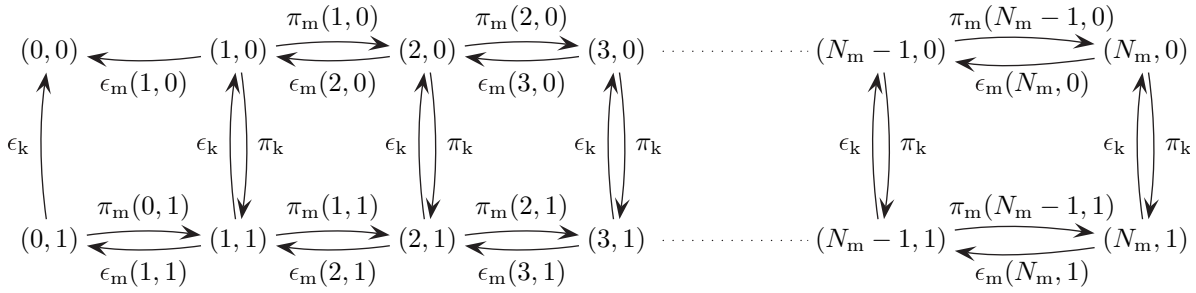

Fig. 4: State space of a cargo particle with one kinesin and N_m myosins.

the simulation are $0.74\,\mu$m/s and $0.36\,\mu$m/s, of similar magnitude as the experimental results $0.73 \pm 0.3\,\mu$m/s and $0.55 \pm 0.15\,\mu$m/s, respectively.

So far, we have assumed that all cargos bind to the microtubule with kinesin first, *i.e.* that the probability w_k for starting a run in the kinesin state $(0,1)$ equals 1. This is reasonable since on one hand we expect that kinesin has a much higher microtubule affinity than the actin-based motor myosin, and on the other hand in the experiments only 28% of all trajectories exhibited diffusive events at all. The latter observation means that w_k must be larger than 0.72. In order to test the influence of whether kinesin or myosin bind first, we repeat our analysis by using the smallest possible value $w_\mathrm{k} = 0.72$. In our procedure, the only rates, $\hat{\epsilon}_\mathrm{m}$ and $\hat{\pi}_\mathrm{m}$, depending on w_k are changed to $\hat{\epsilon}_\mathrm{m} \simeq 0.053\,/$s and $\hat{\pi}_\mathrm{m} \simeq 0/$s. Simulations with these new parameters lead to the average velocity $0.70\,\mu$m/s of all runs, and to the average length $8.8\,\mu$m and velocity $0.25\,\mu$m/s of runs with diffusive events. These values are rather similar to those obtained for $w_\mathrm{k} = 1$.

Generalization to several myosins. – We now generalize our model to the case of cargo transport by one kinesin and N_m myosins, which extends the network in fig. 2(a) to the network in fig. 4. In the latter figure, the unbinding and binding rates for a single myosin in the cargo state $(n_\mathrm{m}, n_\mathrm{k})$ with n_m bound myosins and n_k bound kinesins are denoted as $\epsilon_\mathrm{m}(n_\mathrm{m}, n_\mathrm{k})$ and $\pi_\mathrm{m}(n_\mathrm{m}, n_\mathrm{k})$, respectively. As we have seen before, the kinesin unbinding rate is not influenced by the presence of a single myosin, *i.e.* $\hat{\epsilon}_\mathrm{k} = \epsilon_\mathrm{k}$. We argued that this equality reflects the very low friction of myosin motion on the microtubule. Therefore, we assume that the kinesin unbinding rate remains equal to ϵ_k even if several myosins are bound.

Since an unbound motor is under no force, we take the binding rate of a single motor to be equal to its single-motor binding rate, compare ref. [8]. This assumption implies that the binding rate of kinesin is $\pi_\mathrm{k} \equiv \hat{\pi}_\mathrm{k}$, independent of the number of bound myosins, and that the rate for binding of one of the $(N_\mathrm{m} - n_\mathrm{m})$ unbound myosins in state $(n_\mathrm{m}, n_\mathrm{k})$ is $\pi_\mathrm{m}(n_\mathrm{m}, n_\mathrm{k}) \equiv (N_\mathrm{m} - n_\mathrm{m})\pi_\mathrm{m}$, with $\pi_\mathrm{m} \equiv \hat{\pi}_\mathrm{m}$. Likewise, the unbinding rate of one of the n_m bound myosins in state $(n_\mathrm{m}, 0)$ without bound kinesin is $\epsilon_\mathrm{m}(n_\mathrm{m}, 0) = n_\mathrm{m}\epsilon_\mathrm{m}$.

We have seen above that the unbinding rate of myosin changes from the single-motor unbinding rate ϵ_m to $\hat{\epsilon}_\mathrm{m} > \epsilon_\mathrm{m}$ when one kinesin is bound to the microtubule. To model this effect we consider the motion of a myosin head pulled along by kinesin as diffusion in a moving potential generated by the walking kinesin. Since the myosin and kinesin head are connected via the two motor tails and a rigid cargo, we can approximate this potential by a harmonic spring potential with spring constant K. Because the two motor tails are in series, $1/K \equiv 1/K_\mathrm{m} + 1/K_\mathrm{k}$, where K_m and K_k are the spring constants for the myosin and the kinesin tail, respectively, which are both of the order of $0.3\,$pN/nm [21–23]. We can thus consider the motion of the myosin head as diffusion in a harmonic potential with friction coefficient γ_m, which is reminiscent of the motion of a single motor in an optical trap. This leads to a Gaussian distribution of the spring extension l with average $\langle l \rangle = v_\mathrm{k}\gamma_\mathrm{m}/K$, as required by mechanical equilibrium, and variance $\mathrm{var}[l] = k_\mathrm{B}T/K$ [24]. Hence, the average force $K\langle l \rangle \simeq 0.02\,$pN is negligible, but the force fluctuations $K\sqrt{\mathrm{var}[l]} \simeq 0.8\,$pN are comparably large. Note that a force of $0.8\,$pN is a small force for kinesin with a stall force of 6–7 pN [14,15], but a large force for myosin with a stall force of $2\,$pN [25] (on actin). If myosin feels the force F, its unbinding rate is $\epsilon_\mathrm{m}\exp(F/F_\mathrm{d,m})$ [26], which defines its detachment force $F_\mathrm{d,m}$. Averaging this rate over the Gaussian force distribution, we obtain

$$\epsilon_\mathrm{m}(1,1) = \langle \epsilon_\mathrm{m} \exp[F/F_\mathrm{d,m}] \rangle = \epsilon_\mathrm{m} \langle \exp[Kl/F_\mathrm{d,m}] \rangle = \epsilon_\mathrm{m} \exp\left[(Kk_\mathrm{B}T + 2F_\mathrm{d,m}\gamma_\mathrm{m}v_\mathrm{k})/2F_\mathrm{d,m}^2\right]. \quad (13)$$

Using the experimentally determined values for v_k, ϵ_m and $\epsilon_\mathrm{m}(1,1) = \hat{\epsilon}_\mathrm{m}$ as given in table 1, $K = 0.15\,$pN/nm, and $\gamma_\mathrm{m} = 0.02\,$pNs/nm, we obtain the detachment force $F_\mathrm{d,m} \simeq 0.4\,$pN of myosin on a microtubule.

If there are n_m bound myosins pulled along by one kinesin, we can consider the myosins as n_m springs in parallel, so that the effective spring constant of the system is given via $1/K[n_\mathrm{m}] = 1/(n_\mathrm{m}K_\mathrm{m}) + 1/K_\mathrm{k}$, and the unbinding rate for one myosin is

$$\epsilon_\mathrm{m}(n_\mathrm{m}, 1) = n_\mathrm{m}\epsilon_\mathrm{m} \exp\left[\frac{(K(n_\mathrm{m})k_\mathrm{B}T + 2F_\mathrm{d,m}\gamma_\mathrm{m}v_\mathrm{k})}{2F_\mathrm{d,m}^2}\right]. \quad (14)$$

We simulated a cargo transported by one kinesin and N_{m} myosins with the rates listed in table 1. One quantity of interest is the cargo run length, which increases with the number N_{m} of myosins. For large N_{m}, the run length obtained from the simulations can be fitted by an exponential function. This exponential increase leads to run lengths of the order of $100\,\mu$m, already for 2 or 3 myosins, which is large compared to the single-motor run length of a few μm.

We also studied a non-cooperative model with unbinding rates $\epsilon_{\mathrm{m}}(n_{\mathrm{m}}, 1) = n_{\mathrm{m}}\hat{\epsilon}_{\mathrm{m}}$, which also predicts an exponential increase of the run length. Therefore, such an exponential increase seems to be independent of the precise model for the unbinding rates.

Conclusion. – We present a stochastic model for cooperative cargo transport by actively moving and passively diffusing molecular motors. This model is able to describe the results of recent *in vitro* experiments on cargo transport along a microtubule by one active kinesin-1 and one passive myosin V motor [7]. Our model reproduces the observed increase of the cargo's run length. In our model, the kinesin motion is not influenced by the presence of myosin. In contrast, the unbinding rate of a myosin that is dragged along by kinesin is increased by a factor of 6. We interpret the latter observation within a spring model for the motors: kinesin generates a moving harmonic potential for the myosin, which pulls the myosin along and off the filament.

The generalization of our model to several myosins leads to an exponential increase of the run length, with run lengths of tens of μm for 2 or 3 myosins. Such an exponential increase has previously been found for cargo transport by active motors only [8].

The fact that kinesin remains unimpressed by the presence of myosin while myosin reacts strongly to kinesin's presence is consistent with the general observation that kinesin is a robust microtubule motor [27]. Myosin V is similarly a robust motor on actin filaments, but, compared to kinesin, is only weakly bound to microtubules, and thus can easily be influenced on this filament. This feature is certainly useful for intracellular transport: the passive motor can be easily dragged along without hindering the active motor.

In a very recent *in vitro* experiment [28] the nonprocessive actin motor Myo2p was able to transport a cargo processively on an actin filament, if the kinesin-related protein Smy1p was present on the same cargo. Similar to myosin V in kinesin transport, Smy1p acts as a tether for the nonprocessive motor Myo2p. The latter transport process can be understood by an appropriate modification of our model, as will be described elsewhere.

Although the model that we have presented is for a simple *in vitro* system, it may also provide new insight into the complex traffic *in vivo*. It is certainly tempting to think that, by attaching both actin and microtubule based motors to a cargo, the cell could kill two birds with one stone: the cargo is able to switch between both kinds of tracks, and has an increased run length which prevents it from falling off either of its tracks.

REFERENCES

[1] Howard J., *Mechanics of Motor Proteins and the Cytoskeleton* (Sinauer Associates, Sunderland, Mass.) 2001.
[2] Mallik R. and Gross S. P., *Curr. Biol.*, **14** (2004) R971.
[3] Langford G. M., *Curr. Opin. Cell Biol.*, **7** (1995) 82.
[4] Brown S. S., *Annu. Rev. Cell Dev. Biol.*, **15** (1999) 63.
[5] Goode B. L., Drubin D. G. and Barnes G., *Curr. Opin. Cell Biol.*, **12** (2000) 63.
[6] Ali M. Y., Krementsova E. B., Kennedy G. G., Mahaffy R., Pollard T. D., Trybus K. M. and Warshaw D. M., *Proc. Natl. Acad. Sci. U.S.A.*, **104** (2007) 4332.
[7] Ali M. Y., Lu H., Bookwalter C. S., Warshaw D. M. and Trybus K. M., *Proc. Natl. Acad. Sci. U.S.A.*, **105** (2008) 4691.
[8] Klumpp S. and Lipowsky R., *Proc. Natl. Acad. Sci. U.S.A.*, **102** (2005) 17284.
[9] Müller M. J. I., Klumpp S. and Lipowsky R., *Proc. Natl. Acad. Sci. U.S.A.*, **105** (2008) 4609.
[10] Müller M. J. I., Klumpp S. and Lipowsky R., *J. Stat. Phys.*, **133** (2008) 1059.
[11] Lipowsky R., Klumpp S. and Nieuwenhuizen T. M., *Phys. Rev. Lett.*, **87** (2001) 108101.
[12] Smith D. A. and Simmons R. M., *Biophys. J.*, **80** (2001) 45.
[13] Parmeggiani A., Franosch T. and Frey E., *Phys. Rev. Lett.*, **90** (2003) 086601.
[14] Carter N. J. and Cross R. A., *Nature*, **435** (2005) 308.
[15] Visscher K., Schnitzer M. J. and Block S. M., *Nature*, **400** (1999) 184.
[16] Hill T. L., *Proc. Natl. Acad. Sci. U.S.A.*, **85** (1988) 2879.
[17] Hill T. L., *Proc. Natl. Acad. Sci. U.S.A.*, **85** (1988) 4577.
[18] van Kampen N. G., *Stochastic Processes in Physics and Chemistry* (Elsevier, Amsterdam) 1992.
[19] Hill T. L., *Free Energy Transduction and Biochemical Cycle Kinetics* (Springer, New York) 1989.
[20] Schnakenberg J., *Rev. Mod. Phys.*, **48** (1976) 571.
[21] Veigel C., Schmitz S., Wang F. and Sellers J. R., *Nat. Cell Biol.*, **7** (2005) 861.
[22] Kawaguchi K., Uemura S. and Ishiwata S., *Biophys. J.*, **84** (2003) 1103.
[23] Coppin C. M., Pierce D. W., Hsu L. and Vale R. D., *Proc. Natl. Acad. Sci. U.S.A.*, **94** (1997) 8539.
[24] Astumian R. D., *J. Chem. Phys.*, **126** (2007) 111102.
[25] Mehta A. D., Rock R. S., Rief M., Spudich J. A., Mooseker M. S. and Cheney R. E., *Nature*, **400** (1999) 590.
[26] Bell G. I., *Science*, **200** (1978) 618.
[27] Mallik R. and Gross S. P., *Physica A*, **372** (2006) 65.
[28] Hodges A. R., Bookwalter C. S., Krementsova E. B. and Trybus K. M., *Biophys. J.*, **96** (2009) 546a.